DOE-ET-53088-213 IFSR#213

EFFECTS OF BALLOONING INSTABILITY ON TOKAMAK CONFINEMENT

Guoyong Fu and *J.W. Van Dam*
Institute for Fusion Studies
The University of Texas at Austin
Austin, Texas 78712

May 1987

Effects of Ballooning Instability on Tokamak Confinement

GUOYONG FU and J.W. VAN DAM
Institute for Fusion Studies
The University of Texas at Austin
Austin, Texas 78712

Abstract

Using the ballooning mode transport model proposed by Connor, Taylor, and Turner (1984), we derive the thermal conductivity induced by ideal ballooning instability and compare it to experimental observations from auxiliary-heated tokamaks. We show how this model can be improved by means of a finite-beta equilibrium and also apply it to obtain a confinement scaling law for high-beta, purely ohmically heated tokamaks. Finally, we employ this transport model to find that tokamaks with supplemental stabilization, for example, due to gyroradius, energetic particle, or shaping effects, can self-consistently access the second stability regime at rather high heating power.

1. Introduction

Recently, Connor, Taylor, and Turner (1984) have proposed a simple ballooning mode transport model to explain the observed deterioration of confinement in tokamaks with auxiliary heating. In this model, the thermal conductivity is taken to have the form established for low-beta ohmic discharges wherever the plasma is theoretically stable with respect to ideal MHD ballooning modes. In regions where the plasma is locally unstable to ballooning, the conductivity is considered to be so large that the pressure profile adjusts itself to remain marginally stable. Although quite simple, this model is able to account for a soft beta limit and a gradual degradation of confinement with input power. The significance of this model is that it provides a self-consistent description of profile evolution that incorporates both stability and transport, in contrast to the usual procedure of obtaining an optimized equilibrium profile that is marginally stable at every point.

More recently, this model has been extended (Freidberg & Sigmar 1984; Freidberg, Hakkarainen & Sigmar 1985) to include ohmic, as well as auxiliary, heating effects and to include a phenomenological sawtooth energy convection term to keep the safety factor on axis near unity. Also, they obtained an inverse power scaling for the confinement time in the limit of ultimately large values for the auxiliary heating power.

In a earlier development, Carreras, Diamond, et al. (1983) had proposed that resistive ballooning turbulence is responsible for confinement deterioration in auxiliary heated tokamaks. Their theoretically derived anomalous thermal conductivity agreed quite well with measurements reported for the ISX-B experiment. On the other hand, the energy confinement scaling due to ideal ballooning, as obtained by means of the Connor-Taylor-Turner (CTT) treatment, also seems to agree with experimental results.

In this paper, we propose a method to calculate the anomalous thermal conductivity induced by ideal ballooning instability, based on the CTT model. A comparison of this result with experiment and with the Carreras-Diamond result indicates that the conductivity derived on the basis of the CTT model is in good agreement, but only when a preponderance of the plasma volume is ideally unstable.

Also, we will demonstrate how the CTT model can be improved for high beta plasmas.

The original CTT treatment used a ballooning first stability boundary that is based on a low beta equilibrium model and, hence, is not self-consistent for scaling studies. Here we adopt a high beta equilibrium model developed by Choe and Freidberg (1986) and show how the transport scaling is modified.

Although the CTT theory was focused on auxiliary-heated tokamaks, one may ask whether a similar deterioration occurs for high beta, purely ohmically heated tokamaks. The confinement time of a low beta, ohmically-heated tokamak has been found to be well described by the "benchmark" scaling law $\tau \propto n$, where τ is the energy confinement time and n is the plasma density (Goldston 1984). However, if a tokamak can be ohmically heated to sufficiently high beta values, then ballooning instability may set in, and it is interesting to examine the confinement scaling for this case. Moreover, such a treatment is appealing because of its self-consistent heating profile. Our result, however, indicates that this regime is beyond the operating range of present-day ohmically heated tokamaks.

Finally, we will employ the CTT model to investigate access to the so-called second stability regime (Coppi et al. 1979; Coppi et al. 1980; Greene & Chance 1981) of high beta ballooning modes. Several mechanisms, such as finite Larmor radius effects (Hastie & Hasketh 1981; Tang et al. 1982), pressure anisotropy (Fielding & Haas 1978; Bishop & Hastie 1985), bean-shaped flux surfaces (Miller & Moore 1978; Chance et al. 1983), and the introduction of highly energetic trapped particles (Rosenbluth et al. 1983), can significantly enhance tokamak stability. However, it is not clear whether the plasma can actually pass into the second stability regime self-consistently. Our assessment of this question shows that such access is possible, but only at rather high heating power.

The remainder of the paper is organized in the following manner. In Sec. 2, we review the CTT ballooning mode transport model, with particular attention to the behavior of the plasma profile evolution at large values for the heating power. In Sec. 3, we calculate the anomalous thermal conductivity based on this model and compare it with experiment. In Sec. 4, we obtain a modified CTT confinement scaling by using a high beta tokamak equilibrium model. In Sec. 5, we consider the degradation in confinement for a high beta, ohmically-heated tokamak without auxiliary heating. In Sec. 6 we investigate the question of accessibility to second stability. Finally, Sec. 7 summarizes our conclusions.

2. Profile Evolution at Large Heating Power

First, let us briefly review the ballooning mode transport model developed by Connor, Taylor, and Turner (1984). In their treatment, the plasma is divided into three zones: a sawtooth zone inside the $q = 1$ surface where q is the usual safety factor, a transport zone, and a ballooning zone where the plasma would be linearly unstable. For the sake of simplicity, in this paper we will neglect the sawtooth effects.

Then, in the transport zone, the pressure profile is determined by the thermal conduction equation,

$$\frac{1}{x}\frac{d}{dx}\left[x\frac{d\tilde{p}(x)}{dx}\right] + \frac{1}{\lambda}h(x) = 0, \tag{1}$$

and the poloidal magnetic field is determined by Ampere's equation and Ohm's law,

$$\frac{1}{x}\frac{d}{dx}[xb(x)] = \tilde{p}^{3/2}(x)\left[\int_0^1 dx\ x\ \tilde{p}^{3/2}(x)\right]^{-1}. \tag{2}$$

Equations (1) and (2) are written in the large-aspect-ratio cylindrical approximation with dimensionless variables: $x = r/a$ is the minor radius normalized to the plasma radius a; $\tilde{p}(x) = p(r)/p(0)$ is the normalized scalar plasma pressure; $b(x) = B_\theta(r)/B_\theta(a)$ is the normalized poloidal magnetic field; $h(x)$ is related to the heating power density, normalized so that $\int_0^1 h(x)xdx = 1$; and λ plays the role of an eigenvalue that is adjusted to satisfy the boundary condition that the pressure vanish at the edge of the plasma, $\tilde{p}(1) = 0$. Specifically, the parameter λ is related to the energy confinement time, τ, by the relationship

$$\lambda = c(\tau/\tau_I)\left[\int_0^1 dx\ x\ \tilde{p}^{3/2}\right]^{-1} \tag{3}$$

where $c = \left[1 - \int_0^1 h(x)x^3dx\right]\Big/4$ is related to the heating profile and $\tau_I = 3ca^2/2\chi_I$ is the INTOR confinement time which is associated with the thermal conductivity $\chi_I(m^2/\sec) = 5 \times 10^{19}n^{-1}(m^{-3})$ for ohmic discharges without ballooning instabilities.

In the ballooning zone, the pressure gradient is determined by the condition for ideal MHD ballooning stability,

$$\alpha \equiv -\frac{A\lambda x^2}{b^2(x)}\frac{d\tilde{p}}{dx} = f(S). \tag{4}$$

Here α is essentially the local poloidal beta value multiplied by the inverse aspect ratio: $\alpha = -(2\mu_0 R q^2/B_T^2)(dp/dr)$ in unnormalized form ($\mu_0 = 4\pi \times 10^{-7}$), with R the major radius and B_T the toroidal field. The parameter A is directly proportional to the total input power P:

$$A = 4Pa\tau_I/3cI_p^2R^2\mu_0 = 3.2 \times 10^{-20} \frac{P(MW)a^3(m)n(m^{-3})}{I_p^2(MA)R^2(m)}, \tag{5}$$

where $I_p = 2\pi a B_\theta(a)/\mu_0$ is the plasma current. The right-hand side of Eq. (4), $f(S)$, represents the marginal first stability boundary, which is a function only of the shear $S = b\ d(x/b)/dx$. In the ballooning zone, the poloidal field $b(x)$ is still determined by Eq. (2).

The transport zone extends from $x = 0$ to $x = x_0$, where x_0 is the marginal stability point at which the solutions for $\tilde{p}(x)$ and $b(x)$ in this zone first satisfy $\alpha(x_0) = f(S)$. The ballooning zone then extends from $x = x_0$ to $x = 1$. The boundary conditions are that $d\tilde{p}/dx = 0$ at $x = 0$ and $\tilde{p} = 0$ at $x = 1$. Note that $b = 0$ at $x = 0$ and $b = 1$ at $x = 1$, by definition. For a fixed value of the parameter A, the system of Eqs. (1), (2), and (4) then constitutes an eigenvalue problem with λ as the eigenvalue and $\tilde{p}$ and b as the eigenfunctions. (Note that our neglect of sawtooth effects eliminates $q(a)$ as a parameter.)

We propose to solve this coupled set of eigen-equations by means of a two-eigenvalue shooting method. That is to say, in addition to the eigenvalue λ, we introduce the quantity $\kappa = \int_0^1 x\tilde{p}^{3/2}dx$ as another eigenvalue. Both λ and κ are to be determined for a given value of A, as follows. For arbitrary λ and κ, we obtain $\tilde{p}(x)$ and $b(x)$ in the stable region by integrating Eqs. (1) and (2) in parallel from $x = 0$ up to $x = x_0$ and subsequently in the unstable region by integrating Eqs. (2) and (4) from $x = x_0$ up to $x = 1$. In general, the resulting profiles will not satisfy $p = 0$ and $b = 1$ at the plasma edge. Therefore, we use a shooting method with two loops. In the outer loop, we choose a value for λ; in the inner loop we vary κ until the condition $b(1) = 1$ is satisfied; then the value for λ is changed, and the inner loop is repeated. By means of the outer loop adjustments to λ, we are able to search for a profile that satisfies $\tilde{p}(1) = 0$. Ultimately, of course, the results from this two-eigenvalue scheme will be equivalent to those obtained by iterating on the profiles. (Connor et al. 1984).

The effect of various heating profiles was examined by Connor et al. (1984), who

found that the saturated beta values are relatively independent of the heating profile. In this work, therefore, we will for convenience assume uniform heat deposition and adopt a constant profile for the heating power density: $h(x) = 2$. We then note that Eqs. (1) and (2) in the stable transport region can immediately be integrated to give

$$\tilde{p}(x) = 1 - x^2/2\lambda \quad \text{for} \quad 0 \leq x \leq x_0 \tag{6}$$

and

$$b(x) = \left(\frac{2\lambda}{5\kappa x}\right)\left[1 - \left(1 - \frac{x^2}{2\lambda}\right)^{5/2}\right] \quad \text{for} \quad 0 \leq x \leq x_0. \tag{7}$$

Also note that $c = 1/8$ in this case. Following the two-eigenvalue shooting procedure previously described, we then only need to use numerical integration for Eqs. (4) and (2) in the ballooning region, $x_0 \leq x \leq 1$, where we employ a fourth-order Runge-Kutta method.

As a result of doing so, we are able to reproduce the CTT result that for $A \gtrsim 4.4$, the confinement scaling is well represented by $\tau \propto A^{-0.72}$. We find, moreover, that this scaling remains valid at very large heating powers, at least up to $A = 85.4$.

Figure 1 displays, for various values of A, the profile trajectories of the plasma, plotted as implicit functions of radius in the two-dimensional space of shear versus α, which is a measure of the local pressure gradient. That is to say, the minor radius increases along each trajectory away from the $S - \alpha$ origin, which corresponds to the magnetic axis $x = 0$. The point where the trajectory intersects the marginal stability curve corresponds to the point $x = x_0$ where the ballooning zone begins. As this intersection point drops down the marginal boundary curve, the size of the ballooning zone expands. Figure 1 clearly demonstrates that, as the value of A is increased, the unstable volume of the plasma at first expands rapidly for small A. However, at larger A, this rate of expansion slows down, until at $A \cong 80$, it expands very little. It is precisely due to this feature of the self-consistent evolutionary behavior that the validity of the CTT scaling law survives even at very large heating powers. Consequently, this result indicates that it is nearly impossible to have an inverse power scaling, $\tau \propto A^{-1}$, as has been suggested in Ref. 3. Such an inverse scaling derives directly from Eq. (4) if one were to assume that the entire plasma volume is ballooning marginally unstable. However, the boundary condition $d\tilde{p}/dx \to 0$ at $x = 0$ tends to prevent this situation for all but unreasonably large heating powers.

3. Anomalous Thermal Conductivity Induced by Ideal Ballooning Instability

We now propose to employ the CTT model in order to calculate the anomalous thermal conductivity that would be induced by ideal MHD ballooning modes. Assuming that the thermal conductivity $\chi(r)$ is continuous over the entire plasma volume, we can write down the transport equation for all radii:

$$\frac{1}{x}\frac{d}{dx}\left(\frac{\chi(x)}{\chi_I}x\frac{d\tilde{p}}{dx}\right)+\frac{1}{\lambda}\,h(x)=0. \tag{8}$$

In the ballooning-stable transport region, we have $\chi=\chi_I$ by assumption, and the $\tilde{p}$ and b profiles can be obtained. In the ballooning-unstable regions, we do not *a priori* know the form of χ. Hence, in the style of the CTT approach, we rely on the first stability condition, Eq. (4), to obtain the profiles in that region. For given A, then, eventually one obtains $\lambda(A)$, $\tilde{p}(x,A)$, and $b(x,A)$.

On the other hand, once the profiles are known, we can return to the transport equation, Eq. (8), and integrate it *a posteriori* to obtain the thermal conductivity also in the unstable region. Thus, we have

$$\frac{\chi(x,A)}{\chi_I}=-\frac{\int_0^x xh(x)dx}{\lambda(A)x\partial\tilde{p}(x,A)/\partial x}, \tag{9}$$

with λ and $\tilde{p}$ now as known quantities.

Figures 2 and 3 display the results of calculating the anomalous thermal conductivity in this way for the parameter values $a=0.27\ m$, $R=0.93\ m$, and $n=7\times10^{13}cm^{-3}$ corresponding to two typical high-poloidal-beta discharges in the ISX-B tokamak (Carreras et al. 1983). For the case shown in Fig. 2, the beam power and plasma current were measured to be $P_b=2\ MW$ and $I_p=83\ kA$, respectively. Through Eq. (3), these values correspond to $A=14.8$. Figure 2 shows that our result for χ coincides with that calculated by Carreras and Diamond (1983) on the basis of resistive ballooning turbulence and also agrees fairly well with the experimental conductivity over the effective confinement region $(1<q<2)$.

The case shown in Fig. 3 had $P_\perp = 0.6\ MW$ and $I_p = 143\ kA$, corresponding to $A = 1.5$. Our calculated χ agrees with neither the Carreras-Diamond result nor the experimental result. The reason for the discrepancy is that the case of Fig. 3 had a relatively low beta value: the volume-averaged poloidal beta was $\beta_p = 0.85$. Hence the ideally unstable volume of the plasma is small, and resistive ballooning, dominates the transport.

Nevertheless, in the case corresponding to Fig. 2, the beta value is relatively high ($\beta_p = 1.7$), so that the effect of the ideal ballooning modes is prevalent, because a large portion of plasma volume is ideally unstable. Then the thermal conductivity induced by ideal ballooning modes can represent the experimental results about as well as does the Carreras-Diamond result.

4. Modified Confinement Scaling for Finite Beta

The original CTT theory was based on a low-beta tokamak equilibrium model. In this section we consider how the theory can be improved for high beta plasmas.

Recently, a high beta equilibrium for tokamaks has been proposed by Choe and Freidberg (1986), in which the flux surfaces are assumed to be circular but have a finite Shafranov shift due to the plasma beta. According to their model, the previous low-beta first stability boundary $\alpha = f(S)$ of Eq. (4) is modified to become $\alpha = f(S, \delta)$, where the quantity δ is given by

$$\delta(x) = \frac{3^{3/2}}{2xb^2(x)} \int_0^x dx' b^2(x') \alpha(x'). \tag{10}$$

From the plots of $f(S, \delta)$ given in Choe and Freidberg (1986) for certain fixed values of δ, we note that, to a fair approximation,

$$f(S, \delta) \approx f(S) + \delta/4, \tag{11}$$

which provides us with $f(S, \delta)$ as a continuous function of δ. This expression in Eq. (11) holds when $S \geq 0.5$ (i.e., A not too large) and also $S \geq \alpha$.

Using this high-beta equilibrium and the same method as before, we obtain a modified CTT scaling law,

$$\tau \propto A^{-0.62}, \tag{12}$$

which is shown in Fig. 4, in comparison to the low-beta CTT scaling of $\tau \propto A^{-0.72}$. With the high-beta equilibrium, confinement is therefore improved. This result is clearly related to the stabilizing effect of the Shafranov shift for finite beta.

5. Confinement Scaling for Ohmically Heated, High Beta Plasma

The energy confinement time for a low beta, ohmically heated tokamak generally increases linearly with the density, the so-called INTOR scaling (Goldston 1984). The CTT model (Connor et al. 1984) derived the confinement scaling for a high-beta, purely auxiliary-heated tokamak, and a hybrid treatment of ohmic effects combined with auxiliary heating has been given by Freidberg et al. (1985). We now consider how confinement may be degraded by ideal ballooning modes in a high-beta, purely ohmically-heated tokamak plasma.

With the assumption of pure ohmic heating, the heating density profile can be treated self-consistently as

$$H(r) = E_z J_z = E_z^2/\eta \propto p^{3/2}(r), \tag{13}$$

in contrast to the auxiliary heating case of Sec. II where the heating power profile is independent of the plasma profile. In Eq. (13), we use Spitzer resistivity (Spitzer 1962), which for a hydrogen plasma is given by

$$\eta(\mathrm{ohm-m}) = 5.22 \times^{-5} Z\ \ell n\Lambda/T_e^{3/2}(e\mathrm{V}). \tag{14}$$

Using $p = 2nT$, we write

$$\eta = \eta_0[n/p(0)]^{3/2}\tilde{p}^{-3/2}(x),$$

where $\eta_0 = 9.75 \times 10^{-33} Z\ell n\Lambda$ is a constant and we continue to assume uniform density, as in Connor et al. (1984). The normalized heating density in dimensionless units, as in Eq. (1), is given by

$$h(x) = \frac{4\pi^2 Ra^2 H(r)}{P} = \frac{\tilde{p}^{3/2}(x)}{\int_0^1 dx\ x\ \tilde{p}^{3/2}(x)}. \tag{15}$$

Note that the ohmic heating input power, $P = \int d^3r\sigma E_z^2$, can be written as

$$P = 2\pi R I_p E_z, \tag{16}$$

if we use Eq. (2) to relate the current I_p to the electric field E_z and the quantity $\kappa = \int_0^1 dx\ x\ \tilde{p}^{3/2}$:

$$I_p = \frac{2\pi a}{\mu_0} B_\theta(a) = 2\pi a^2 \int_0^1 dx\ x\ \sigma E_z = 2\pi a^2 [p(0)/n]^{3/2} E_z \kappa/\eta_0. \tag{17}$$

As in Sec. 2, we solve self-consistently for the plasma pressure and poloidal field profiles in the ballooning stable and unstable zones, again neglecting sawtooth effects. In the ballooning-stable transport zone, $0 \leq x \leq x_0$, the determining equations are again Eqs. (1) and (2), here rewritten in view of Eq. (15) as

$$\frac{1}{x}\frac{d}{dx}\left(x\frac{d\tilde{p}}{dx}\right) + \frac{\tilde{p}^{3/2}(x)}{\lambda\kappa} = 0 \tag{18}$$

$$\frac{1}{x}\frac{d}{dx}(xb) = \frac{\tilde{p}^{3/2}(x)}{\kappa}. \tag{19}$$

The eigenvalue $\lambda = 4\pi^2 R p(0)\chi_I/P$ is still given by Eq. (3), which can be written as $\lambda\kappa = c(\tau/\tau_I)$, with the constant c defined as before but with the $h(x)$ of Eq. (15). In the marginally unstable zone, $x_0 \leq x \leq 1$, the pressure gradient is determined by the ideal stability condition of Eq. (4), in conjunction with Eq. (19) for the field. However, we rewrite Eq. (4) in terms of a scaling parameter A' that involves neither $p(0)$ nor E_z, since for ohmic heating we desire a confinement scaling that depends on n, I_p, and R. This objective is satisfied by rewriting Eq. (4) in the form

$$-A'(\lambda/\kappa)^{2/5}\ \frac{x^2}{b^2}\ \frac{d\tilde{p}}{dx} = f(S), \tag{20}$$

with the scaling parameter given by

$$A' = 5.52 \times 10^{-21} n(m^{-3}) a^{2.2}(m) R^{-1}(m) I_p^{-1.2}(MA). \tag{21}$$

The results of solving the system of Eqs. (18)-(20), again by a two-eigenvalue method, are shown in Fig. 5. For $A' > 1$, we obtain the confinement $\tau/\tau_I \propto A'^{-0.44}$, or

$$\tau \propto a^{1.03} n^{0.56} R^{0.44} I_p^{0.53}. \tag{22}$$

It is interesting to see whether the saturation point ($A' \approx 1$) is relevant to contemporary ohmically heated tokamaks. For example, Alcator C ($a = 0.165\ m$, $R = 0.64\ m$,

$I_p = 0.5\ MA$) is an ohmically heated tokamak with fairly high densities. The point where $A' = 1$ then corresponds to a critical density of $n_c \cong 2.7 \times 10^{15}\ cm^{-3}$, which is beyond the usual operating range of Alcator C. From this we conclude that confinement deterioration due to the ballooning instability has little effect in purely ohmically heated tokamaks.

6. Accessibility to Second Stability

The question of accessibility to the second stability regime for ballooning modes is a subtle one. In general, it is studied under the assumption of a given plasma profile. That is to say, one assumes profiles for, say, the normalized pressure $\beta = \beta_0\hat{\beta}(\psi)$ and the safety factor $q = q_0\hat{q}(\psi)$, solves the Grad-Shafranov equilibrium equation for the flux ψ, and determines the linear stability boundary in (β_0, q_0) parameter space. The claim, then, is that the plasma can access second stability along any path that does not intersect the unstable region. However, this type of approach has the intrinsic defect of not being self-consistent, since it assumes a certain profile. In this section, we propose to address the accessibility issue by means of the CTT method, which, although oversimplified, does allow for a self-consistent determination of the plasma profile.

Let us recall that in the ideal MHD theory of ballooning modes, accessibility is prevented by an unstable gap that separates the regions of first and second stability. (We do not consider the case where the plasma may be able to penetrate this gap by very rapid heating (Tuda et al. (1981).) However, tokamak stability can be significantly enhanced by the introduction of certain supplemental stabilizing mechanisms. For example, the effects of finite gyroradius (Hastie & Hasketh 1981; Tang et al. 1982) and pressure anisotropy (Fielding & Haas 1978; Bishop & Hastie 1985) can be taken into account, the plasma cross-section can be bean-shaped (Miller & Moore 1979; Chance et al. 1983) or highly energetic trapped particles could be injected (Rosenbluth et al. 1983). For each of these schemes or possibly a combination thereof, with judicious choice of parameters, a direct avenue of accessibility can open up between the first and second stable regions.

For the sake of simplicity, we will here represent the enhanced marginal stability boundary in generic form as

$$\alpha_c = f'(S) = 1.2S \pm 0.6\sqrt{S^2 - S_m^2}. \tag{23}$$

Here the α of the toroidal core plasma is designated as α_c, in order to distinguish it, for example, from that for a hot particle component. Figure 6 displays the model marginal curves of Eq. (23), plotted for several values of the parameter S_m, which is a measure of the

supplemental stabilization. For whatever provides the enhancement, the larger the value of S_m, the greater its stabilizing effect. For instance, the curve for $S_m = 0.5$ approximately models the FLR-stabilized boundary (Tang et al. 1982) for $k\rho_i = 0.4$; or, the curve for $S_m = 0.9$ is similar to the stability boundary for hot particles trapped with a half-width of $\pi/4$ on the outer side of a tokamak (Rosenbluth et al. 1983). In our analysis, the parameter S_m will be considered to be constant. We caution that S_m is actually not a constant, but is related back to an equilibrium profile. For example, the stability boundary obtained by Rosenbluth et al. (1983) was based on a very special distribution function such that α for the hot particles, α_h, is at each point chosen to have its maximum value as allowed by the condition of non-reversal of the magnetic curvature drift. Hence, the self-consistent determination of S_m is a fairly complicated matter and will be left for future study.

We now propose to use the CTT ballooning transport model described in Sec. 2, but with Eq. (23) in place of Eq. (4). The major difference is that now the ballooning stability boundary bifurcates as a function of the shear. There is a minimum value for the shear, S_m, below which ballooning modes are stable for all values of α_c. This feature allows the possibility of access to second stability. We wish to determine whether access can occur, by calculating the $S - \alpha_c$ profile evolution and the corresponding confinement time as the auxiliary heating power is adiabatically increased from zero to large values.

The numerical results for the case $S_m = 1.0$ are shown in Fig. 7. As the power (proportional to A) is increased, Fig. 7 shows that the point that divides the stable and unstable portions of the $S - \alpha_c$ trajectory and thus corresponds to $x = x_0$, moves down along the left side of the marginal stability boudary. This indicates that the unstable volume of the plasma expands. At the critical value $A_c \cong 21.0$, this point reaches the nadir of the stability curve, at $S = S_m$. If A is slightly increased beyond its critical value, there is no longer a solution in the first stability region, but a solution exists in the second stability region. The consequence is an abrupt change in the profile evolution and, correspondingly, a jump in the confinement time, which is shown in Fig. 8. Also shown is the situation where the power is reduced, beginning from large values. For very large P, the $S - \alpha_c$ trajectory does not know about the unstable gap since it passes completely under it, and therefore the confinement time settles down to INTOR scaling. As the power is reduced, the trajectory will partially lie along the right side of the stability boundary, with the lower endpoint of

this segment at some $S > S_m$. Because stability increases with beta in the second stability region, the confinement time is slightly enhanced above INTOR confinement. When the power is further reduced, the trajectory reverts abruptly to first stability, thus yielding a hysteresis behavior for confinement.

A comparison of the confinement time scalings for various values of S_m is presented in Fig. 8. The critical power to access second stability from below is given by $A_c \cong 11.5$ for $S_m = 1.3$ and $A_c \cong 21$ for $S_m = 1.0$. The value of A_c obviously has a strong dependence on S_m. Since in practice, as was mentioned previously, the parameter S_m may assure values from approximately 0.5 to 0.9, rather high power would be required for accessibility. This result is seen to be consistent with the statement in Sec. 2 that the CTT scaling remains valid at moderately large heating powers.

Summary

In this work, we have presented some extensions and applications of the ballooning transport model that was proposed by Connor et al. (1984) to study the self-consistent profile evolution and confinement of an auxiliary-heated plasma. We find that the CTT confinement scaling $\tau \propto P^{-0.72}$ remains valid even for extremely large values of the heating power, so that the inverse linear scaling suggested by Freidberg et al. (1985) seems improbable. It was shown that the anomalous thermal conductivity induced by ideal ballooning modes can be obtained in this model and that it compares well with both the experimental result and the theoretical result of Carreras and Diamond (1983) at high beta, but not so well at low beta where the resistive modes are dominant. The simplicity of the CTT model, which is its strength, thus also restricts its validity. For high beta, it was also shown that use of a semi-analytic improved equilibrium (Choe & Freidberg 1986) leads to a slightly improved prediction for the confinement time.

We also applied the CTT method to study confinement in a high beta, purely ohmically heated tokamak. The results indicate that confinement degradation would set in at rather high values. Therefore, ideal ballooning appears to have little influence on ohmic confinement.

Finally, we applied the method to study accessibility to the second stability regime for ballooning modes, with the result that rather large input power would be required. This treatment was not entirely self-consistent. However, it may indicate that experiments aimed at attaining second stability should consider a variety of schemes, including non-adiabatic heating scenarios.

Acknowledgments

The authors gratefully acknowledge Dr. P.H. Diamond for suggesting consideration of the second stability accessibility problem; Profs. M.N. Rosenbluth, J.P. Freidberg, and R.H. Hazeltine for useful discussions; and Dr. M. Murakami for some ISX-B experimental data.

REFERENCES

BISHOP, C.M. & HASTIE, R.J. 1985 Annual Controlled Fusion Theory Meeting (Madison, Wisconsin, 15-17 April), paper 1R2.

CARRERAS, B.A., DIAMOND, P.H., MURAKAMI, M., DUNLAP, J.L., BELL, J.D., HICKS, H.R., HOLMES, J.A., LAZARUS, E.A., PARÉ, V.K., SIMILON, P., THOMAS, C.E. & WIELAND, R.M. 1983 Phys. Rev. Lett. **50**, 503.

CHANCE, M.S., JARDIN, S.C. & STIX, T.H. 1983 Phys. Rev. Lett. **51**, 1963.

CHOE, W.H. & FREIDBERG, J.P. 1986 Phys. Fluids **29**, 1766.

CONNOR, J.W., TAYLOR, J.B. & TURNER, M.F. 1984 Nucl. Fusion **24**, 642.

COPPI, B., FERREIRA, A., MARK, J.W.-K. & RAMOS, J.J. 1979 Nucl. Fusion **19**, 715.

COPPI, B., FERREIRA, A. & RAMOS, J.J. 1980 Phys. Rev. Lett. **44**, 990.

FIELDING, P.J. & HAAS, F.A. 1978 Phys. Rev. Lett. **41**, 801.

FREIDBERG, J.P. & SIGMAR, D.J. 1984 Bull. Amer. Phys. Soc. **29**, 370.

FREIDBERG, J.P., HAKKARAINEN, S.P. & SIGMAR, D.J. 1985 Annual Controlled Fusion Theory Meeting (Madison, Wisconsin, 15-17 April), paper 2B4.

GOLDSTON, R.J. 1984 Plasma Phys. and Controlled Fusion **26**, 87.

GREENE, J.M. & CHANCE, M.S. 1981 Nucl. Fusion **21**, 453.

HASTIE, R.J. & HESKETH, K.W. 1981 Nucl. Fusion **21**, 651.

MILLER, R.L. & MOORE, R.W. 1979 Phys. Rev. Lett. **43**, 765.

ROSENBLUTH, M.N., TSAI, S.T., VAN DAM, J.W. & ENGQUIST, M.G. 1983 Phys. Rev. Lett. **51**, 1967.

SPITZER, L. JR. 1962 *Physics of Fully Ionized Gases* (Interscience Publishers, New York, Second Revised Edition), p. 139.

TANG, W.M., DEWAR, R.L. & MANICKAM, J. 1982 Nucl. Fusion **22**, 1081.

TUDA, T., AZUMI, M., KURITA, G., TAKIZUKA, T. & TAKEDA, T. 1981 *Report* JAERI-M 9472, Japan Atomic Energy Research Institute.

Figure Captions

1. Plasma profiles of shear versus pressure gradient, for increasing values of the heating power.

2. High beta radial profiles of the ISX-B experimental, Carreras-Diamond, and ideal ballooning thermal conductivities.

3. Low beta radial profiles of the ISX-B experimental, Carreras-Diamond, and ideal ballooning thermal conductivities.

4. Dependence of the confinement time on input power, for a high beta model tokamak equilibrium.

5. (a) Dependence of the confinement time on the input power parameter A' for a purely ohmically heated plasma. (b) Logarithmic dependence of the confinement time, for $A' \geq 1$.

6. Model stability boundary for a tokamak with supplemental stabilization whose effectiveness is characterized by S_m.

7. Plasma profiles of shear versus pressure gradient, for increasing values of the input power, with the model stability boundary ($S_m = 1.0$).

8. Hysteresis dependence of the confinement time on input power, with the model stability boundary ($S_m = 1.5$).

9. Comparison of the confinement time scaling with power for various values of S_m (increasing power only).

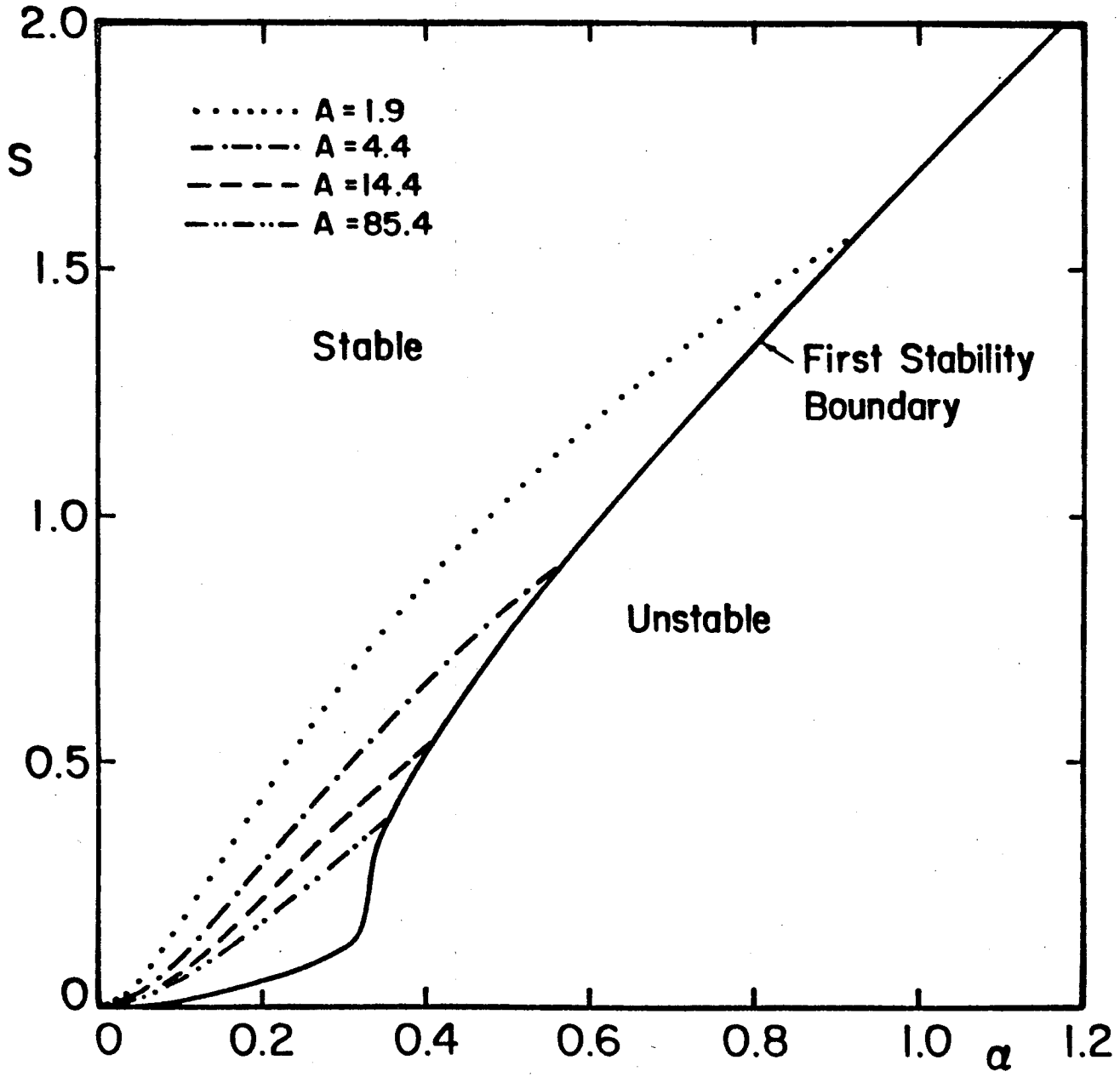
2.0
1.5
1.0
0.5
0
S
A = 1.9
A = 4.4
A = 14.4
A = 85.4
Stable
Unstable
First Stability
Boundary
0
0.2
0.4
0.6
0.8
1.0
1.2
α

Fig. 1

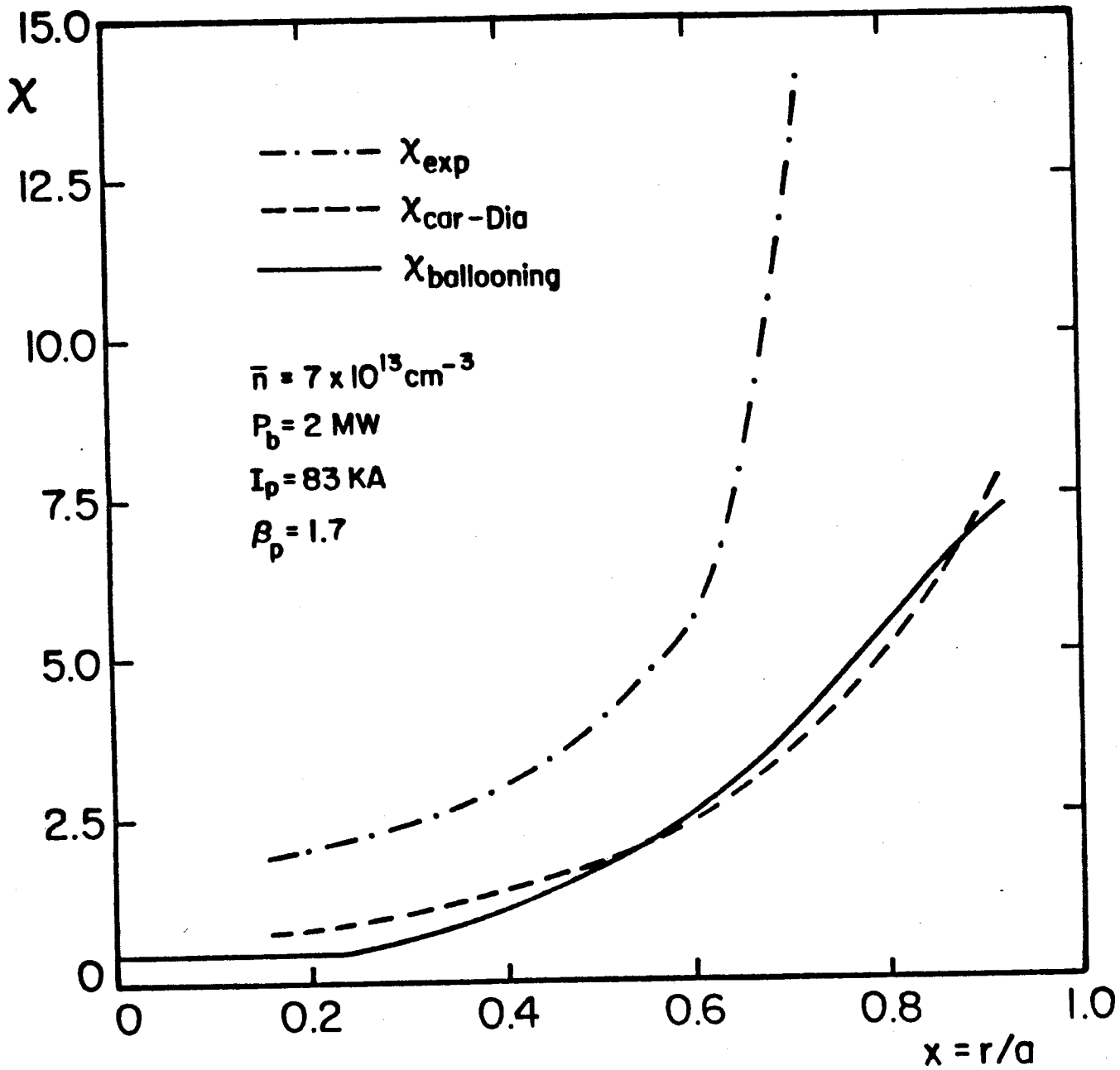
15.0
χ
12.5
10.0
7.5
5.0
2.5
0
0
0.2
0.4
0.6
0.8
1.0
x = r/a
χ_{exp}
$\chi_{car-Dia}$
$\chi_{ballooning}$
$\bar{n} = 7 \times 10^{13} cm^{-3}$
$P_b = 2$ MW
$I_p = 83$ KA
$\beta_p = 1.7$

Fig. 2

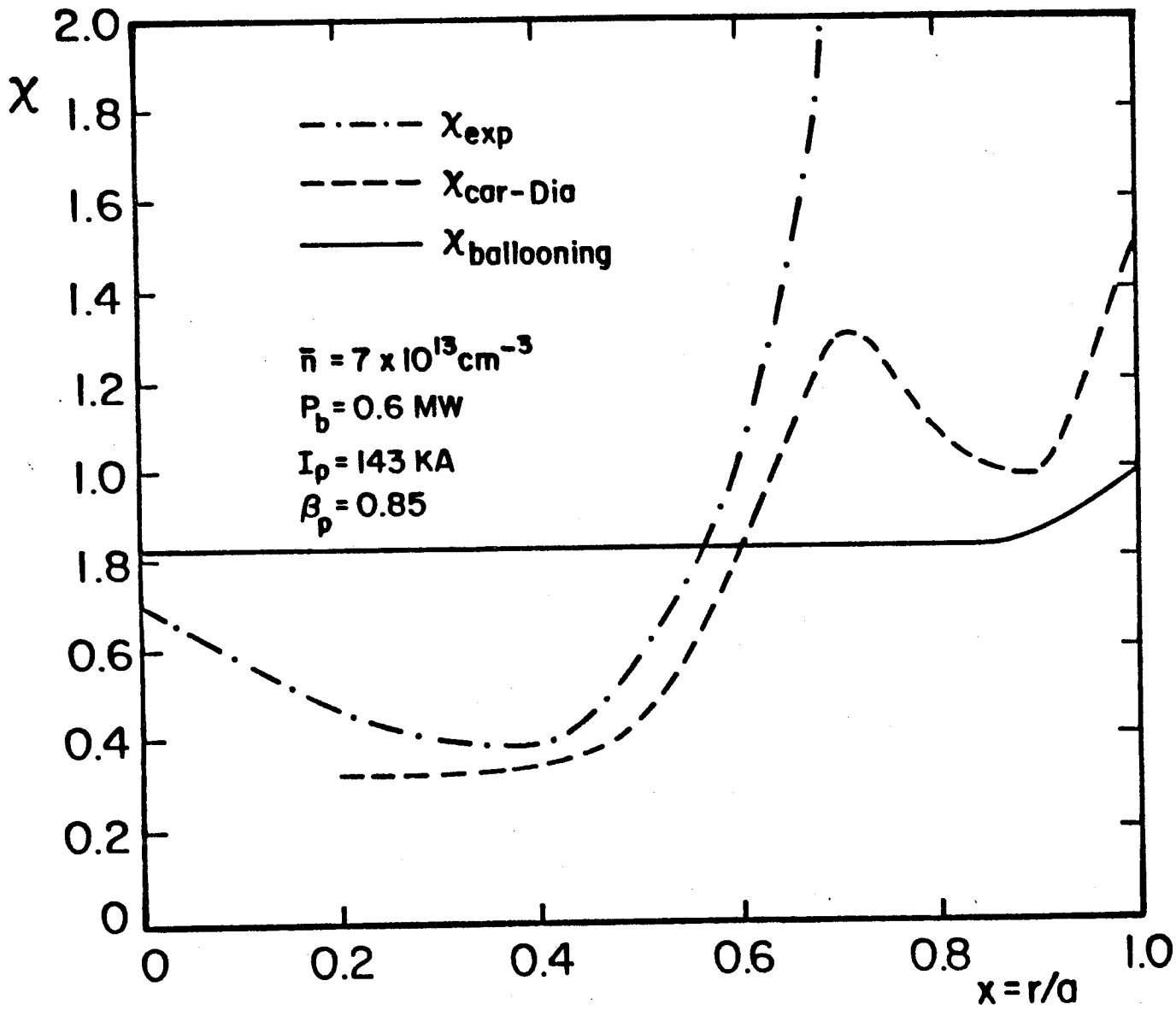
χ
2.0
1.8
1.6
1.4
1.2
1.0
1.8
0.6
0.4
0.2
0
0
0.2
0.4
0.6
0.8
1.0
x = r/a
χexp
χcar-Dia
χballooning
n̄ = 7 x 10^13 cm^-3
Pb = 0.6 MW
Ip = 143 KA
βp = 0.85

Fig. 3

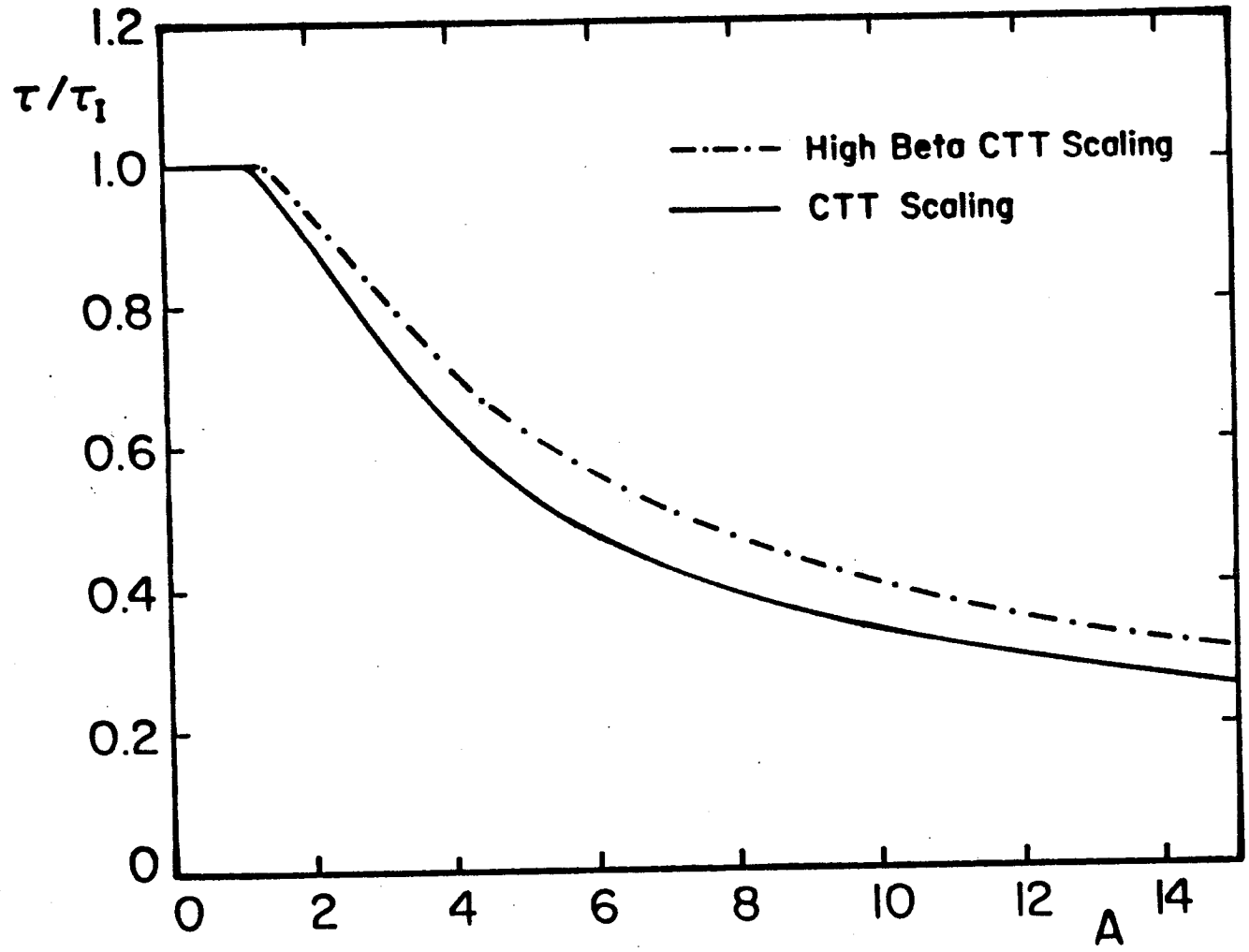
1.2
τ/τ_I
1.0
0.8
0.6
0.4
0.2
0
0
2
4
6
8
10
12
14
A
High Beta CTT Scaling
CTT Scaling

Fig. 4

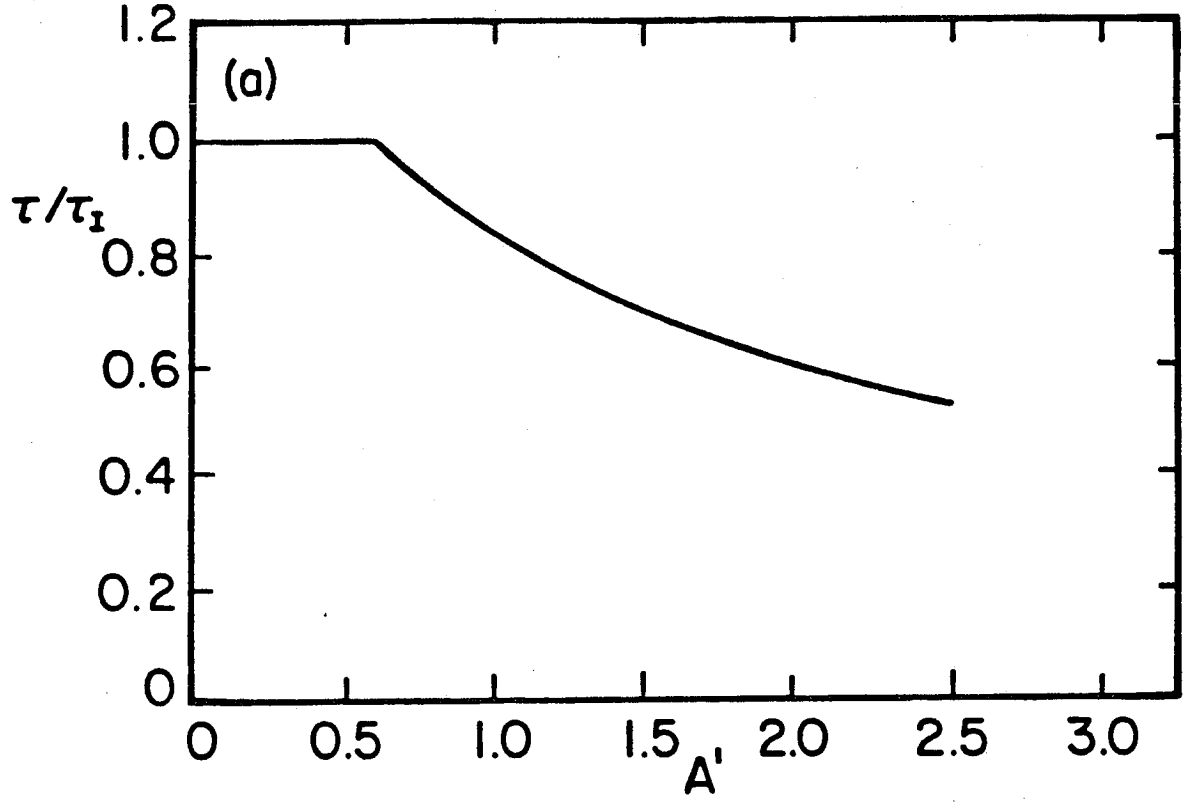
(a)
1.2
1.0
0.8
0.6
0.4
0.2
0
τ/τ_I
0
0.5
1.0
1.5
2.0
2.5
3.0
A'

Fig. 5(a)

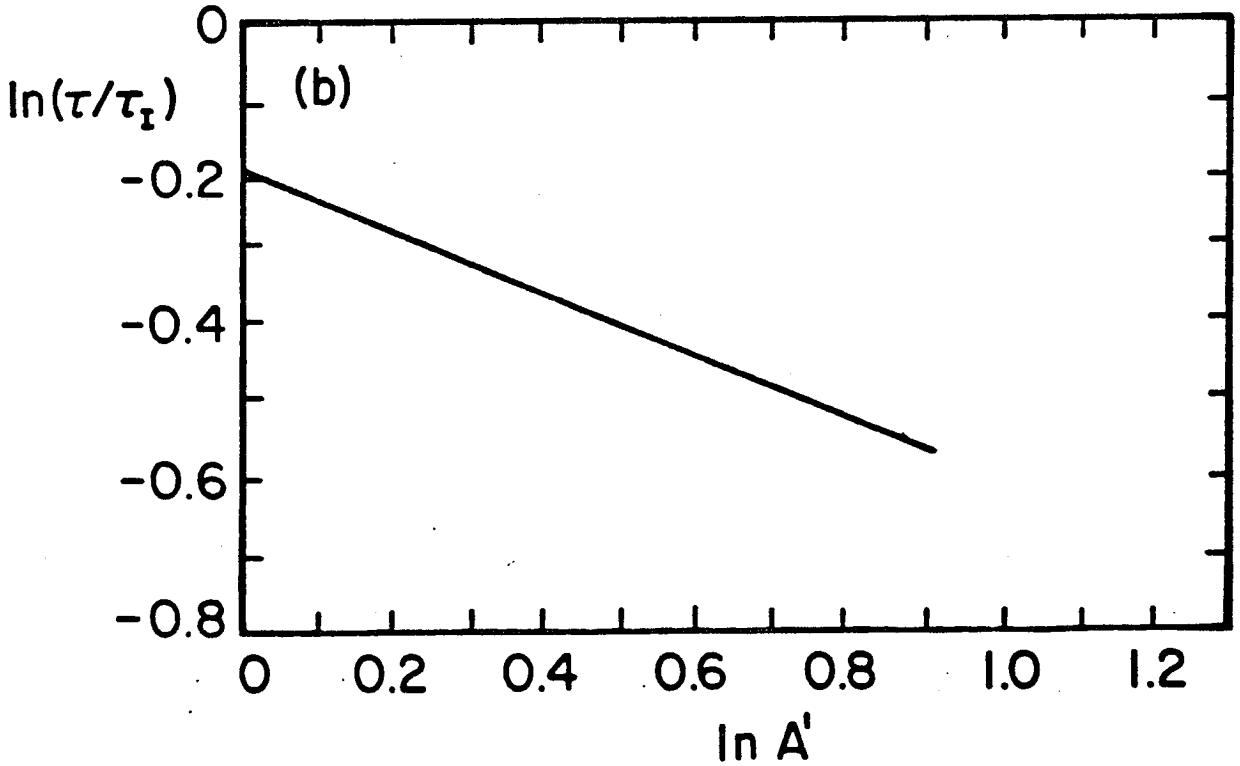
(b)
0
-0.2
-0.4
-0.6
-0.8
ln(τ/τ_I)
0
0.2
0.4
0.6
0.8
1.0
1.2
ln A'

Fig. 5(b)

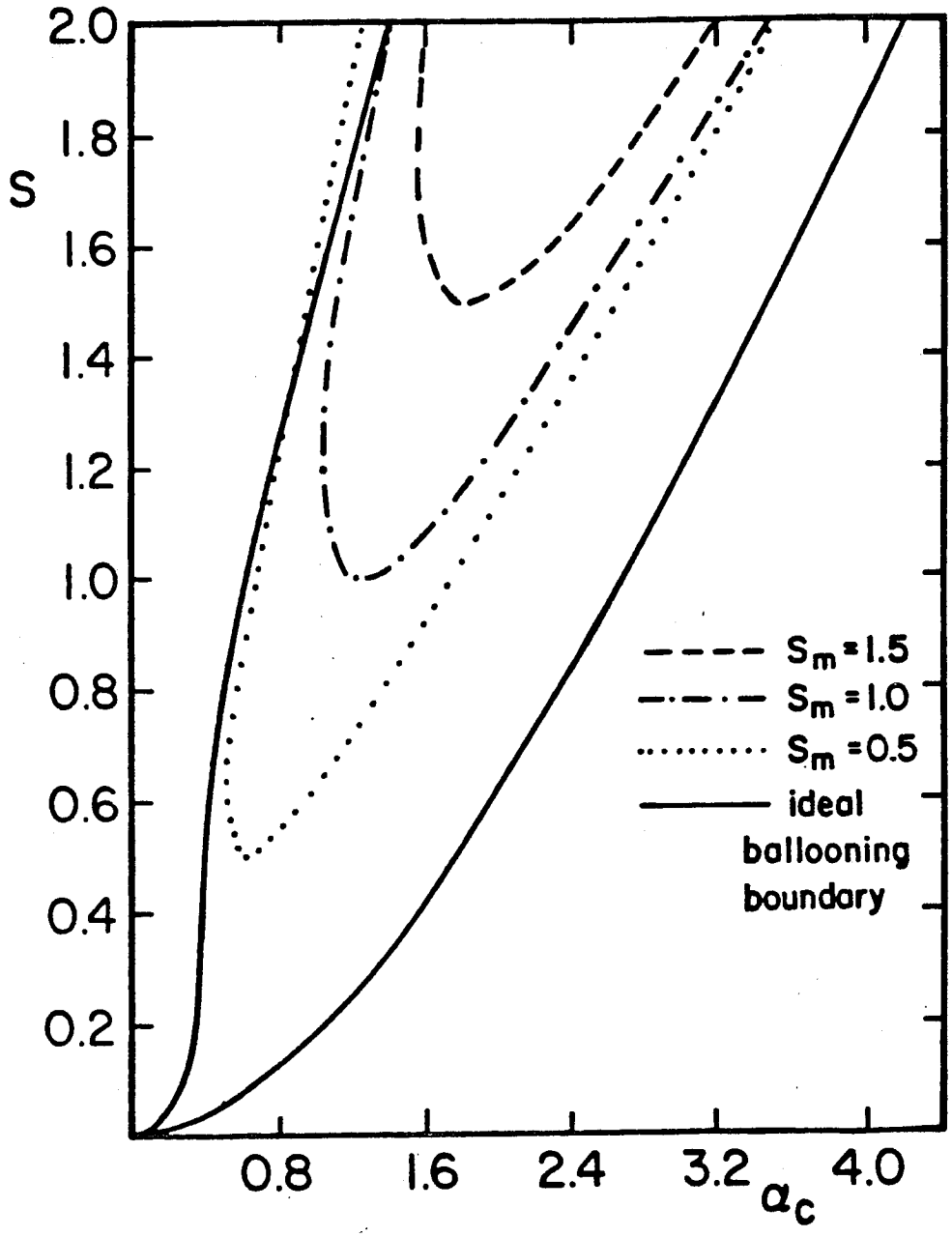
2.0
1.8
1.6
1.4
1.2
1.0
0.8
0.6
0.4
0.2
S
0.8
1.6
2.4
3.2
4.0
α_c
$S_m = 1.5$
$S_m = 1.0$
$S_m = 0.5$
ideal ballooning boundary

Fig. 6

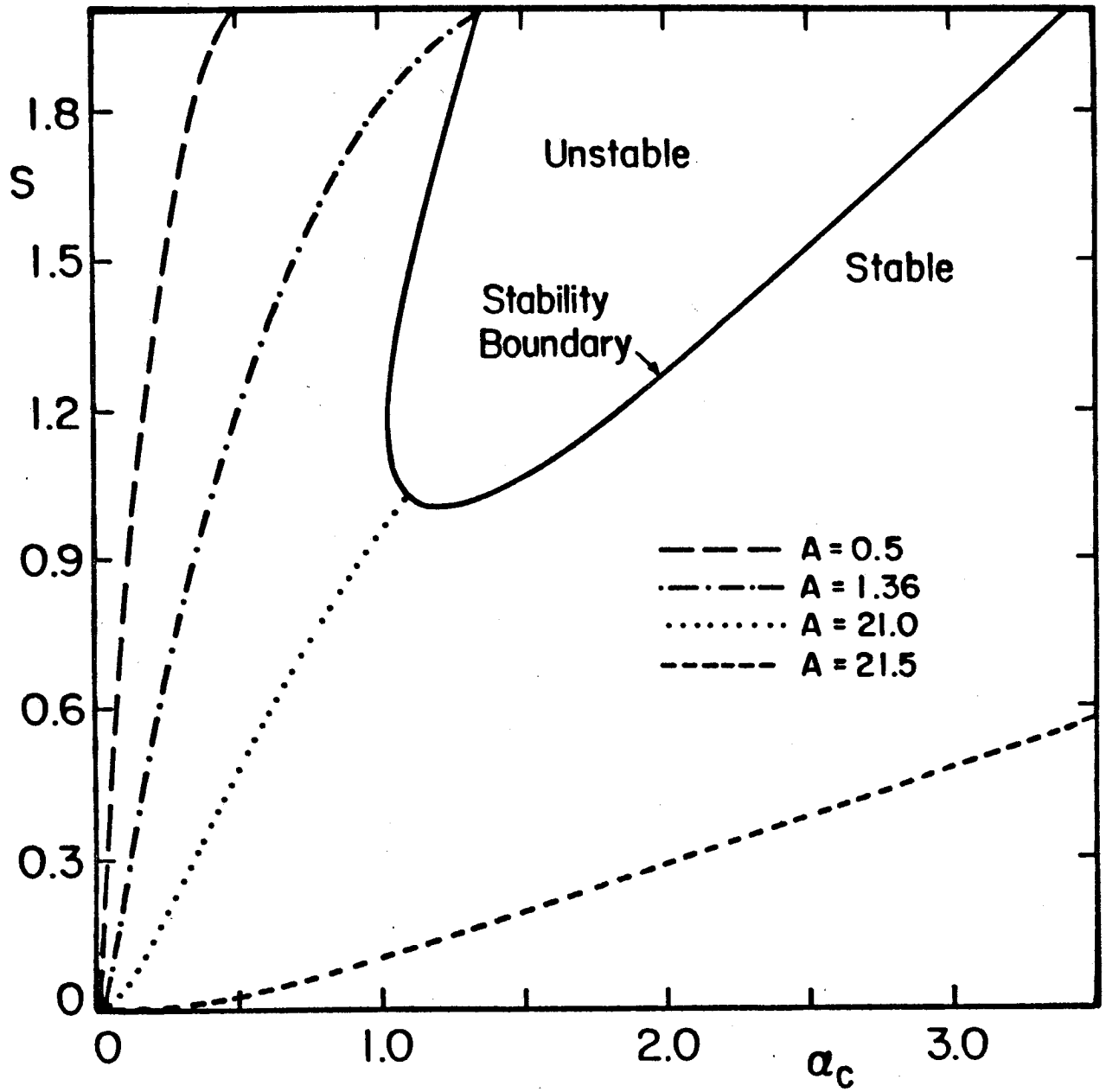
1.8
S
1.5
1.2
0.9
0.6
0.3
0
0
1.0
2.0
3.0
α_c
Unstable
Stable
Stability
Boundary
A = 0.5
A = 1.36
A = 21.0
A = 21.5

Fig. 7

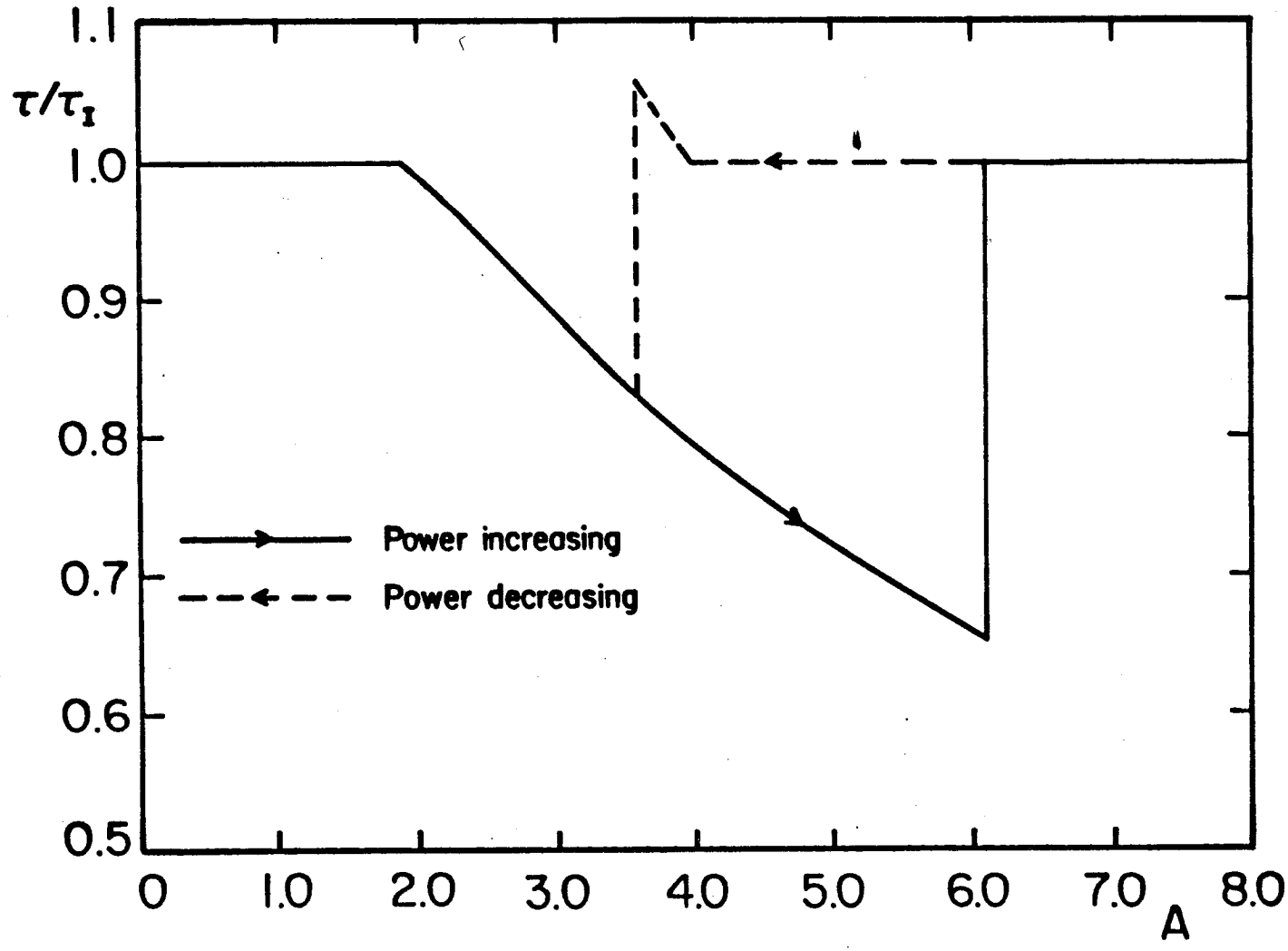
1.1
τ/τ_I
1.0
0.9
0.8
0.7
0.6
0.5
0
1.0
2.0
3.0
4.0
5.0
6.0
7.0
8.0
A
Power increasing
Power decreasing

Fig. 8

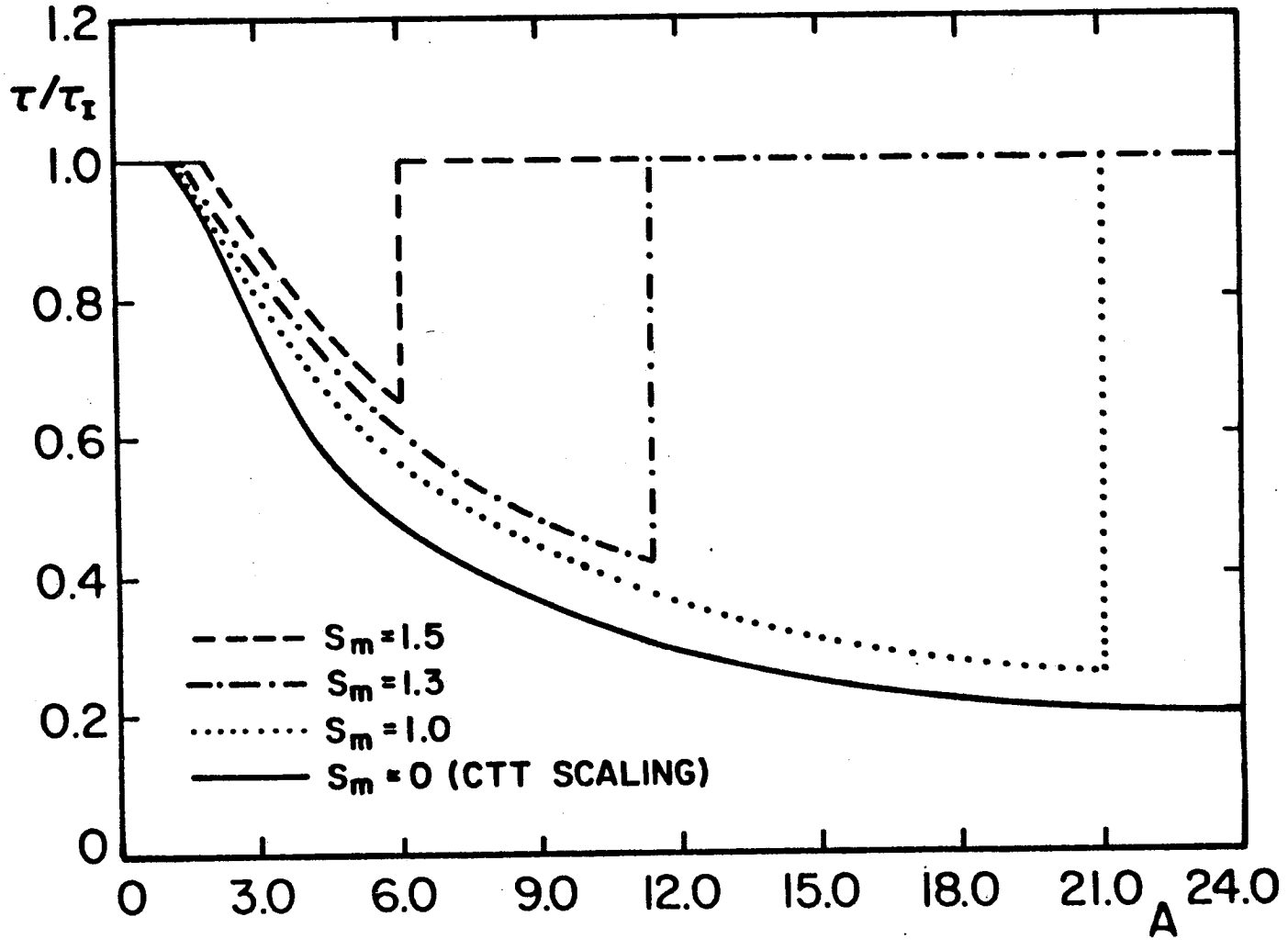
1.2
τ/τ_I
1.0
0.8
0.6
0.4
0.2
0
0
3.0
6.0
9.0
12.0
15.0
18.0
21.0
24.0
A
S_m = 1.5
S_m = 1.3
S_m = 1.0
S_m = 0 (CTT SCALING)

Fig. 9